

Radial Restricted Solid-on-Solid and Etching Interface Growth Models

Sidiney G. Alves*

*Departamento de Física e Matemática,
Universidade Federal de São João Del-Rei
36420-000, Ouro Branco, MG, Brazil*

In this work an approach to generate radial interfaces is presented. A radial network recursively obtained is used to implement discrete model rules designed originally for the investigation in flat substrates. In order to test the proposed scheme, we have used the restricted solid-on-solid and etching models. The results indicate the KPZ conjecture is fully verified. Besides, a very good agreement between the interface radius fluctuation distribution and the GUE one was observed. The evolution of the radius agrees very well with the generalized conjecture, and the two-point correlation function exhibits a very good agreement with the covariance of Airy₂ process. So, this approach can be used to investigate radial interfaces evolution for others universality classes.

PACS numbers: 68.43.Hn, 68.35.Fx, 81.15.Aa, 05.40.-a

I. INTRODUCTION

Fluctuations are inherent to far from equilibrium phenomena, and are present in a broad range of growing systems in nature, from thin film deposition to biological growth. These fluctuations are characterized by self-similarity and universality that emerge from distinct dynamical processes of their formation [1, 2]. A large number of non-equilibrium fluctuations phenomena are associated to the universality class of the equation proposed by Kardar, Parisi, and Zhang (KPZ) [3]

$$\frac{\partial h(x,t)}{\partial t} = \nu \nabla^2 h(x,t) + \lambda (\nabla h(x,t))^2 + \eta(x,t) \quad (1)$$

where $h(x,t)$ represents the interface height at a position x in time t , the first term in the right hand corresponds to surface tension, the non-linear second term represents a local lateral growth in the normal direction along the surface and the last one is a white noise with $\langle \eta(x,t) \rangle = 0$ and $\langle \eta(x,t) \eta(x',t') \rangle = D \delta(x-x') \delta(t-t')$.

In the last two decades, we witnessed an increase in the interest to the KPZ universality class due to the exact results obtained for 1 + 1 dimensions [4, 5]. The central point of these exact results is that the height fluctuations of interfaces belonging to the KPZ universality class can be described by Tracy-Widom distributions. The fluctuation probability distribution function depends on the substrate geometry or initial condition dividing the KPZ universality in different sub-classes. The height evolution of a single site is given by

$$h(t) = v_\infty t + (\Gamma t)^\beta \chi \quad (2)$$

where v_∞ and Γ are system depending parameters, β is the universal growth exponent and χ is a random variable that describes the fluctuations. The probability distribution function of this random variable splits the KPZ universality in two sub-classes depending on the substrate

geometry. In flat substrates, the random variable is associated to the Gaussian orthogonal ensemble distribution, while, in curved substrates, the random variable follows the Gaussian unitary ensemble (GUE) distribution. This conjecture was verified in several analytical (including exact solution) [6–10], experimental [11–14] and numerical [15–19] works for both geometries. The conjecture stated by the equation 2 was extended to high dimensions. Initially in 2 + 1 dimensions, with numerical approaches [19–21] and followed by experimental evidences [22–24]. Later, it was extended to dimensions up to 6 + 1 using numerical simulations of discrete growth models [25, 26].

The conjecture in Eq. (2) was generalized to take into account finite time corrections in the height cumulants observed in various works using analytical [6–9, 27], experimental [11–13] and numerical approaches [16–19, 21, 28]. The generalized version includes additional terms as follows

$$h(t) = v_\infty t + s_\lambda (\Gamma t)^{1/3} \chi + \eta + \zeta t^{-1/3} + \dots \quad (3)$$

here η and ζ are non-universal parameters. Both play an important role at finite-time analyses.

The numerical investigation of interface growth is traditionally based on discrete growth models. The main investigated models belonging to the KPZ universality class are restricted solid-on-solid (RSOS) [29], ballistic deposition [30], single step [31], etching [32] and Eden [33]. In the particular case of a curved substrate, besides all the works mentioned above, the main studies are based on radial interface evolution of the Eden growth model [33] and its variations [18]. On lattice simulations of the radial version exhibits anisotropy effects leading to distorted interfaces with growth velocity varying along the chosen direction. The analysis must be done using fixed directions [18]. Even though the off-lattice radial simulations in 1 + 1 dimension are quite affordable, large scale simulation are expensive [34].

In this work, a method to adapt growth model rules to generate radial interfaces is proposed. The rules of RSOS and etching models were used in a lattice built

*Electronic address: sidiney@ufsj.edu.br

hierarchically. The obtained results for both models indicate a convergence of the universal parameter of KPZ universality class. The KPZ conjecture is fully verified with a very good agreement between the interface radius fluctuation distribution and the GUE one. Besides, the results obtained to the two-point correlation function exhibits a very good agreement with the covariance of the Airy_2 process.

The paper is organized as follows. In the next section, the hierarchical network is described, and the growth rules details are presented. In Sec. III, we present and discuss the results. Section IV is devoted to the conclusions.

II. MODEL

The radial network was built considering a set of circular concentric layers enumerated as $\ell = 0, 1, \dots$. A layer ℓ has a radius r_ℓ and $N_\ell = \text{INT}(2\pi r_\ell)$ sites here the radius $r_\ell = r_0 + \ell$ and $\text{INT}(x)$ is a function to return the value of x truncated. The N_ℓ sites are distributed on the layer ℓ , in a way that its cell has an arc length of unitary size. The site locations are obtained recursively beginning with a random selection of the angular location ϕ_1 of the first one, the remaining sites of the layer are positioned considering $\phi_i = \phi_{i-1} + \delta\phi$ with $i = 2, 3, \dots, N_\ell$ and $\delta\phi = \frac{2\pi r_\ell}{N_\ell}$. The neighborhood of the sites is obtained during the construction process as schematically illustrated in Fig. 1. A new site i at a layer ℓ will be a neighbor of the site $i-1$ at same layer and of those at the inner layer ($\ell-1$). In this case, we search by the sites of $\ell-1$ layer that share an edge with the cell of site i . So, in general, each new site has bonds with three neighbors previously added. Besides, the neighborhood of site $i-1$ and of those on layer $\ell-1$ are updated to store the site i as neighbor. The procedure is repeated to obtain the interested number of layer.

The interface growth rules for RSOS and etching models are implemented considering, as initial condition, all sites of the first layer occupied. The top panel in Fig. 2

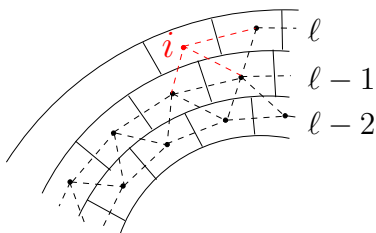


FIG. 1: (Color online) Schematic illustration of the construction of the neighborhood in the radial network. The last added site and the bonds with the site of its layer and of the previous one is highlighted in red. Notice that the bond with the site of the layer and with that of previous layer is identified in the addition.

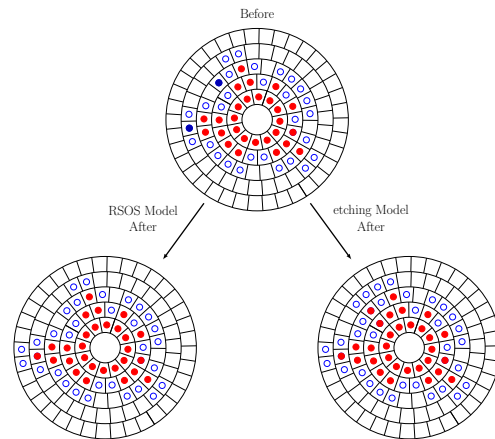


FIG. 2: (Color on-line) Schematic illustration of the growth rules of the RSOS and etching models. The top panel show two chosen sites (blue full circles). Bottom panels show the new configurations using the RSOS (left) and the etching rules (right).

shows an illustration of an interface after few steps. The deposited and peripheral sites are highlighted by red full and blue open circles, respectively. New particles will be deposited on the peripheral sites. The RSOS rules are implemented considering that a new incoming particle will occupy a peripheral site at random. The incorporation of the new particle to the interface must take into account the previous layer. If all neighboring sites of this layer are occupied the deposition is accepted. Otherwise, if the site i has at least one empty neighbor at the previous layer, the deposition is refused. These implementation rules are equivalent to the flat deposition considering the restriction parameter $m = 1$. The etching growth rules are implemented as follows. A deposition site i belonging to the peripheral is chosen. All empty neighbors in previous layers are filled. The update rules for the two models are schematically illustrated in Fig. 2. The upper configuration shows two peripheral sites chosen to deposition (they are highlighted by blue filled circles). The bottom configurations show the interface after the update using RSOS (left) and etching (right) rules. Since we randomly pick up a peripheral site from a constantly updated list containing N_p sites, the time is updated as $t = t + dt$ at each attempt with $dt = 1/N_p$. This strategy to update the time is based on that used in the Eden growth model where only the peripheral sites may divide [16]. The simulations were carried out on networks considering the first radius layer $r_0 = 10$ and the simulations run until the aggregates reach a radius $r = 10^4$. Averages are taken from up to $N = 10^4$ independent samples.

III. RESULTS AND DISCUSSION

The investigation of the radial growth was done considering the time evolution of the interface radius fluctuation.

tuations. The cells belonging to the interface at time t are defined by the set of those adjacent to the peripheral one. As mentioned previously, the radius of an interface cell is defined by its layer, *i.e.*, a cell in the layer ℓ has a radius $r_\ell = r_0 + \ell$.

At short times, the height fluctuation exhibits a behavior with Gaussian distribution as reported previously [35] (results not show). The asymptotic value of the interface growth velocity is obtained considering the time derivative of the first moment. From Eq. (2), it is given by

$$\partial_t \langle h \rangle = v_\infty + s_\lambda \Gamma^\beta \beta t^{\beta-1} \langle \chi \rangle. \quad (4)$$

So, as shown in the upper insets of Fig. 3(a) and 3(b), the value of v_∞ is obtained using a linear fit in the plot of $\partial_t \langle h \rangle$ against $t^{\beta-1}$ here $\beta = 1/3$ was used. The asymptotic values obtained for both, RSOS and etching growth model, are presented in table I. Notice that, considering Eq. 2, the radius second cumulant is given by

$$\langle h^2 \rangle_c = (\Gamma t)^{2\beta} \langle \chi^2 \rangle_c \quad (5)$$

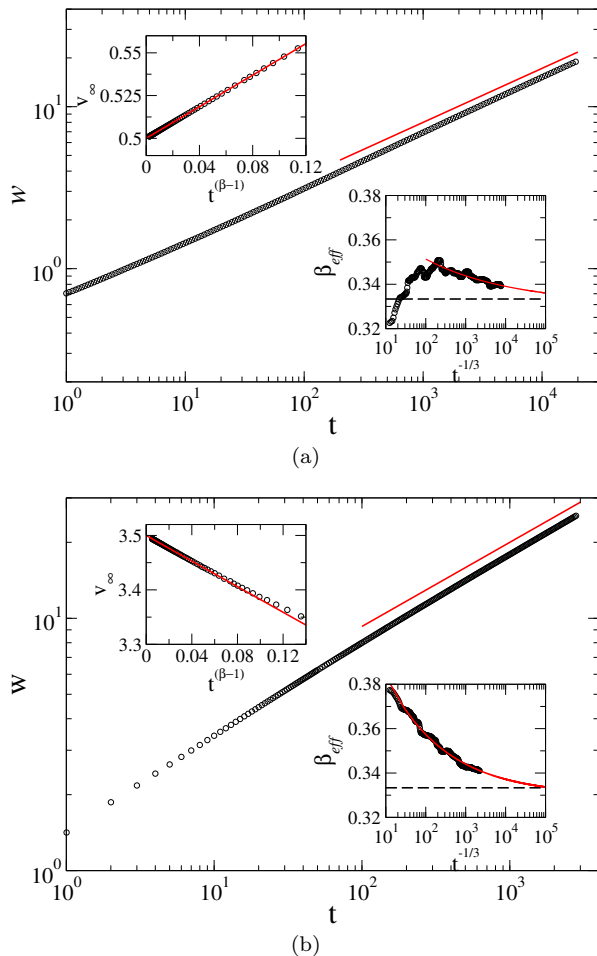


FIG. 3: (Color online) Evolution of the second cumulant of the radius for the RSOS (a) and etching (b) models. Insets show the time derivative of the first (top insets) and of the second (bottom insets) cumulant for the two models.

| | v_∞ | β | Γ_1 | Γ_2 | $\langle \eta \rangle$ | S | K |
|---------|------------|----------|------------|------------|------------------------|---------|----------|
| RSOS | 0.50001(4) | 0.334(3) | 0.49(1) | 0.50(1) | 8.2(2) | 0.22(1) | 0.095(2) |
| etching | 3.49997(3) | 0.331(2) | 8.2(2) | 8.5(3) | 15.4(3) | 0.21(1) | 0.085(5) |

TABLE I: Nonuniversal and universal quantities for the dynamical regime of KPZ models.

The results in main panels of Fig. 3(a) and 3(b) show a clear power law $w = (\langle h^2 \rangle_c)^{1/2}$ vs time for both RSOS and etching models. Bottom insets of these figures show β_{eff} as a function of $t^{-1/3}$. Here, $\beta_{eff} = d(\ln(w))/d(\ln(t))$ gives the local derivative of $\ln w$ versus $\ln t$. For the RSOS model, a non-monotonic behavior is observed. However, in both models the growth exponent asymptotically converges to values very close to $1/3$. The obtained values are presented in table I. In addition, the higher order cumulants were used to obtain the skewness (S) and kurtosis (K) associated to the radius fluctuations, defined as

$$S = \frac{\langle h^3 \rangle_c}{\langle h^2 \rangle_c^{1.5}} \quad (6)$$

$$K = \frac{\langle h^4 \rangle_c}{\langle h^2 \rangle_c^2} \quad (7)$$

The plot of S and K against time exhibits a finite time correction in the convergence to the asymptotic value (results not shown) consistent with a power law convergence with exponent $2/3$. The estimated values are in very good agreement with those associated to the KPZ class (see Table I).

A crucial step is the determination of the parameters λ and Γ to analyze the agreement of the radius fluctuations distribution with the GUE one. In the radial interface growth $\lambda = v_\infty$ and the Γ parameter are derived from Eq. (2) and (5) and reads

$$\Gamma_1^\beta = \frac{\langle h \rangle - v_\infty t}{t^\beta \langle \chi \rangle} \quad (8)$$

$$\Gamma_2^{2\beta} = \frac{\langle h^2 \rangle_c}{t^{2\beta} \langle \chi^2 \rangle_c}, \quad (9)$$

regarding that $\langle \chi \rangle = -1.771069$ and $\langle \chi^2 \rangle_c = 0.812729$ are the first and second cumulants of the GUE distribution. The values of Γ_1 and Γ_2 were obtained using a linear extrapolation in the plot against $t^{-\beta}$ and $t^{-2\beta}$, respectively, as shown in Fig. 4 (solid lines). The estimated values are presented in table I. Note that the values of Γ_1 and Γ_2 are close for both models, so in the next results we consider Γ as a mean of these two values.

Using the estimated parameters in the previous analysis and the Eq. (2) we can calculate the random variable given by

$$q = \frac{\langle h \rangle - v_\infty t}{s_\lambda (\Gamma t)^\beta}. \quad (10)$$

The plot of $q - \langle \chi \rangle$ against $s_\lambda (\Gamma t)^{-\beta}$ is shown in Fig. 5. A clear linear behavior is observed asymptotically. Besides,

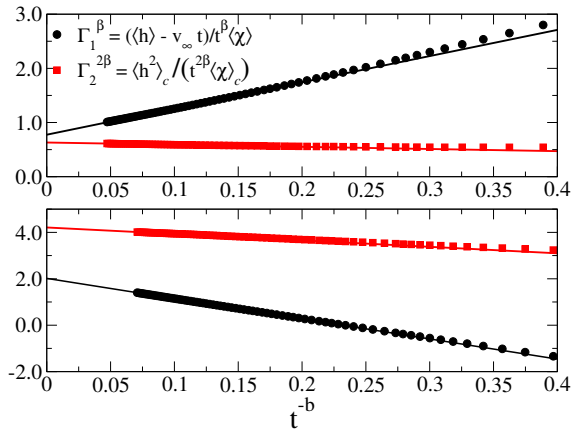


FIG. 4: (Color online) The Γ parameter obtained using the Eq. (8) and (9) for RSOS and etching models, top and bottom, respectively. Here, we set $\langle \chi \rangle = -1.771069$ and $\langle \chi^2 \rangle_c = 0.812729$ and $b = \beta$ and 2β for the Γ_1 and Γ_2 , respectively.

when the evolution from early times is considered, as can be seen from inset in Fig. 5, a very good fit is obtained when a double power law $q - \langle \chi \rangle = at^{-1/3} + bt^{-2/3}$ is used in the plot. This regression was considered previously in numerical simulations [18]. So, the q variable converges to $\langle \chi \rangle$ as

$$q = \langle \chi \rangle + \frac{\langle \eta \rangle}{s_\lambda (\Gamma t)^\beta} + \frac{\langle \zeta \rangle}{s_\lambda \Gamma^\beta t^{2\beta}} \quad (11)$$

as aforementioned, here the second term is associated to a shift in the q variable in relation to the mean value of the GUE distribution and the last term to finite time corrections. In the light of the previous results, the behavior of the radius is in agreement with the generalized KPZ conjecture.

To compare the obtained radius distribution function of RSOS and etching models with the TW-GUE one, the

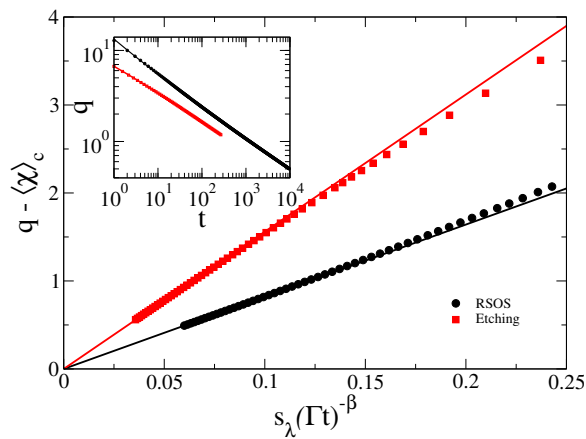


FIG. 5: (Color online) Convergence of the random variable q to $\langle \chi \rangle$ for the two models as shown in the legend. The solid lines are linear fit to the asymptotic regions.

radius can be scaled as

$$q' = \frac{\langle h \rangle - v_\infty t - \langle \eta \rangle}{s_\lambda (\Gamma t)^\beta}. \quad (12)$$

Figures 6(a) and 6(b) show the rescaled probability distribution for RSOS and etching models, respectively. An excellent agreement is observed for the two models.

Finally, the two-point correlation function, given by

$$C_2(\varepsilon, t) = \langle r(x + \varepsilon, t)r(x, t) \rangle - \langle R(x, t) \rangle \quad (13)$$

for radial growth models belonging to the KPZ universality exhibit the scaling $C_2(\varepsilon, t) \approx (\Gamma t)^{2\beta} g_2(u)$ with $u = (A\varepsilon/2)(\Gamma t)^{2\beta}$ and $g_2(u)$ is the covariance of the Airy₂ process [36]. To verify the scaling for the RSOS and etching interfaces we plot in Fig. 7 the two-point correlation function considering the rescale $\tilde{C}_2 = (\Gamma t)^{-2\beta} \times C_2$ against u . A remarkable agreement is observed for the RSOS model while the results for the etching are converging (the time is increased from bottom to top curves as indicated on the legend figure).

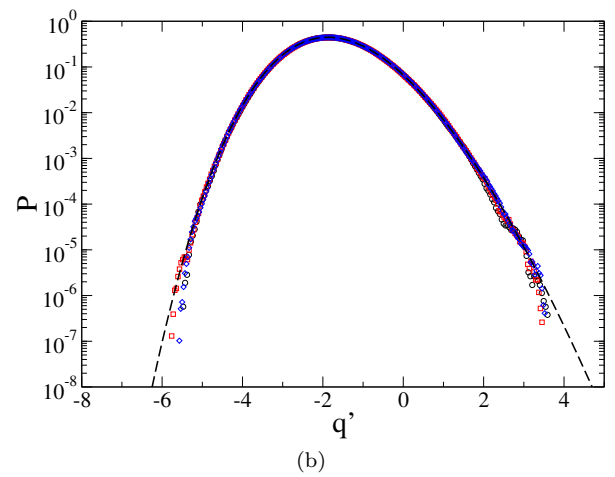
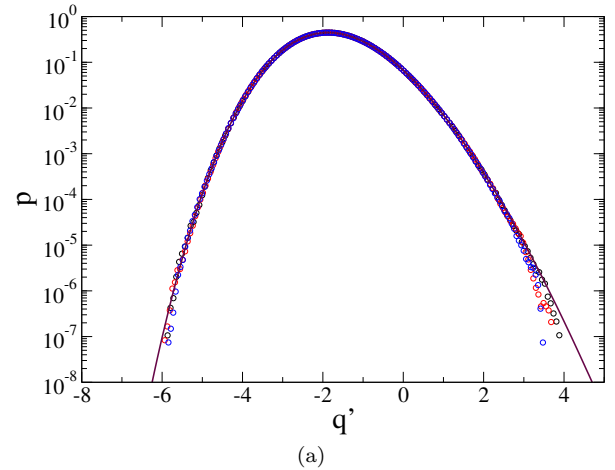


FIG. 6: (Color online) Height distribution function at different times scaled according to the Eq. (12). For the RSOS model we have used $t = 5000, 7500$ and 10^4 while for the etching model, $t = 10^3, 2000$ and 3000 .

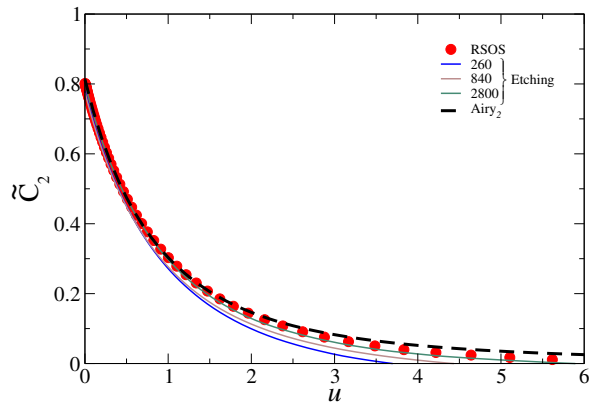


FIG. 7: (Color online) Rescaled two-point correlation function $\tilde{C}_2 = (\Gamma t)^{-2\beta} \times C_2$ against the rescaled length u . The dashed line represents the Airy_2 correlation function.

IV. CONCLUSIONS

In this work, we present a strategy to investigate the discrete interface growth models in radial geometry. The restricted solid-on-solid (RSOS) and etching growth model rules were adapted to generate radial interfaces. The fluctuations of the interface radius was investigated in $1 + 1$ dimensions. The radius moments, growth exponent and universal quantities presented an excellent agreement with those of the KPZ universality class. Besides, the generalized KPZ conjecture was fully verified

with the radius distribution exhibiting a very good agreement with the Tracy-Widom of the Gaussian unitary ensemble, as conjectured to the KPZ universality class for curved surfaces. These findings were corroborated by the quantitative agreement between the RSOS and etching two-point correlation scaling and the Airy_2 process. Recently, quantitative predictions for the universal form of the two-time correlations in the infinite time limit of the KPZ equation were derived [37]. This work shows the breaking of the ergodicity in radial systems time evolution. So, these universal properties will be investigated using the present strategy on a future work. Furthermore, the strategy present here can be used to investigate the interface growth of models belonging to other universality classes. We are working in the implementation of the rule of conserved version of the RSOS and Das Sarma-Tamborenea models, that belong to the nonlinear molecular beam epitaxy universality class. A recent work shows that these models present a dependency on flat (fixed-size) and expanding substrates [38]. The results will appear elsewhere as soon as possible.

Acknowledgements

The author thanks the discussions with Silvio C. Ferreira and for the critical reading of the manuscript by him and Marcelo M. Oliveira. The author also thanks F. Bornemann by kindly providing the covariance of the Airy_2 process. This work was partially supported by CNPq and FAPEMIG (Brazilian agencies).

-
- [1] A.-L. Barabasi and H. E. Stanley, *Fractal Concepts in Surface Growth* (Cambridge University Press, Cambridge, England, 1995).
- [2] P. Meakin, *Fractals, Scaling and Growth far from Equilibrium* (Cambridge University Press, Cambridge, England, 1998).
- [3] M. Kardar, G. Parisi, and Y.-C. Zhang, *Phys. Rev. Lett.* **56**, 889 (1986).
- [4] K. Johansson, *Commun. Math. Phys.* **209**, 437 (2000).
- [5] M. Prähofer and H. Spohn, *Phys. Rev. Lett.* **84**, 4882 (2000).
- [6] T. Sasamoto and H. Spohn, *Phys. Rev. Lett.* **104**, 230602 (2010).
- [7] T. Sasamoto and H. Spohn, *J. Stat. Mech.: Theor. Exp.* **2010**, P11013 (2010).
- [8] G. Amir, I. Corwin, and J. Quastel, *Commun. Pure Appl. Math.* **64**, 466 (2011).
- [9] P. Calabrese and P. Le Doussal, *Phys. Rev. Lett.* **106**, 250603 (2011).
- [10] T. Imamura and T. Sasamoto, *Phys. Rev. Lett.* **108**, 190603 (2012).
- [11] K. A. Takeuchi and M. Sano, *Phys. Rev. Lett.* **104**, 230601 (2010).
- [12] K. A. Takeuchi, M. Sano, T. Sasamoto, and H. Spohn, *Sci. Rep.* **1**, 34 (2011).
- [13] K. A. Takeuchi and M. Sano, *Journal of Statistical Physics* **147**, 853 (2012).
- [14] P. J. Yunker, M. A. Lohr, T. Still, A. Borodin, D. J. Durian, and A. G. Yodh, *Phys. Rev. Lett.* **110**, 035501 (2013).
- [15] J. Rambeau and G. Schehr, *EPL (Europhysics Letters)* **91**, 60006 (2010).
- [16] S. G. Alves, T. J. Oliveira, and S. C. Ferreira, *Europhys. Lett.* **96**, 48003 (2011).
- [17] T. J. Oliveira, S. C. Ferreira, and S. G. Alves, *Phys. Rev. E* **85**, 010601 (2012).
- [18] S. G. Alves, T. J. Oliveira, and S. C. Ferreira, *Journal of Statistical Mechanics: Theory and Experiment* **2013**, P05007 (2013).
- [19] S. G. Alves, T. J. Oliveira, and S. C. Ferreira, *Phys. Rev. E* **90**, 052405 (2014).
- [20] T. Halpin-Healy, *Phys. Rev. Lett.* **109**, 170602 (2012).
- [21] T. J. Oliveira, S. G. Alves, and S. C. Ferreira, *Phys. Rev. E* **87**, 040102 (2013).
- [22] T. Halpin-Healy and G. Palasantzas, *Europhys. Lett.* **105**, 50001 (2014).
- [23] R. A. L. Almeida, S. O. Ferreira, T. J. Oliveira, and F. D. A. Aarão Reis, *Phys. Rev. B* **89**, 045309 (2014).

- [24] R. A. L. Almeida, S. O. Ferreira, I. R. B. Ribeiro, and T. J. Oliveira, *Europhys. Lett.* **109**, 46003 (2015).
- [25] S. G. Alves, T. J. Oliveira, and S. C. Ferreira, *Phys. Rev. E* **90**, 020103(R) (2014).
- [26] S. G. Alves and S. C. Ferreira, *Phys. Rev. E* **93**, 052131 (2016).
- [27] P. Ferrari and R. Frings, *J. Stat. Phys.* **144**, 1 (2011).
- [28] K. A. Takeuchi, *J. Stat. Mech.* **2012**, P05007 (2012).
- [29] J. M. Kim and J. M. Kosterlitz, *Phys. Rev. Lett.* **62**, 2289 (1989).
- [30] M. J. Vold, *Journal of Colloid Science* **14**, 168 (1959), ISSN 0095-8522.
- [31] P. Meakin, P. Ramanlal, L. M. Sander, and R. C. Ball, *Phys. Rev. A* **34**, 5091 (1986).
- [32] B. A. Mello, A. S. Chaves, and F. A. Oliveira, *Phys. Rev. E* **63**, 041113 (2001).
- [33] M. Eden, in Proceedings of Fourth Berkeley Symposium on Mathematics, Statistics, and Probability, edited by J. Neyman (University of California Press, Berkeley, California, 1961), vol. 4, pp. 223–239.
- [34] S. G. Alves, S. C. Ferreira, and M. L. Martins, *Braz. J. Phys.* **38**, 81 (2008).
- [35] S. Prohac and H. Spohn, *Phys. Rev. E* **84**, 011119 (2011).
- [36] F. P. Bornemann F. and Prähofer, *J. Stat. Phys.* **133**, 405 (2008).
- [37] J. De Nardis, P. Le Doussal, and K. A. Takeuchi, *Phys. Rev. Lett.* **118**, 125701 (2017).
- [38] I. S. S. Carrasco and T. J. Oliveira, *Phys. Rev. E* **94**, 050801(R) (2016).